Received: 10 August 2023 | Revised: 22 December 2023 | Accepted: 26 February 2024

DOI: 10.1002/hbm.26655

RESEARCH ARTICLE

WILEY

The transition from vision to language: Distinct patterns of functional connectivity for subregions of the visual word form area

Maya Yablonski[1,2] | Iliana I. Karipidis[3,4,5] | Emily Kubota[6] | Jason D. Yeatman[1,2,6]

[1]Division of Developmental-Behavioral Pediatrics, Department of Pediatrics, Stanford University School of Medicine, Stanford, California, USA

[2]Stanford University Graduate School of Education, Stanford, California, USA

[3]Department of Psychiatry and Behavioral Sciences, Stanford School of Medicine, Stanford, California, USA

[4]Department of Child and Adolescent Psychiatry and Psychotherapy, University Hospital of Psychiatry Zurich, University of Zurich, Zürich, Switzerland

[5]Neuroscience Center Zurich, University of Zurich and ETH, Zurich, Switzerland

[6]Psychology Department, Stanford University, Stanford, California, USA

Correspondence
Maya Yablonski, Division of Developmental-Behavioral Pediatrics, Department of Pediatrics, Stanford University School of Medicine, Stanford, CA, USA.
Email: mayay@stanford.edu

Funding information
National Science Foundation, Grant/Award Number: DGE-1656518; Stanford Maternal and Child Health Research Institute; Zuckerman-CHE STEM leadership program; National Institute of Child Health and Human Development, Grant/Award Number: R01-HD095861

Abstract

Reading entails transforming visual symbols to sound and meaning. This process depends on specialized circuitry in the visual cortex, the visual word form area (VWFA). Recent findings suggest that this text-selective cortex comprises at least two distinct subregions: the more posterior VWFA-1 is sensitive to visual features, while the more anterior VWFA-2 processes higher level language information. Here, we explore whether these two subregions also exhibit different patterns of functional connectivity. To this end, we capitalize on two complementary datasets: Using the Natural Scenes Dataset (NSD), we identify text-selective responses in high-quality 7T adult data ($N = 8$), and investigate functional connectivity patterns of VWFA-1 and VWFA-2 at the individual level. We then turn to the Healthy Brain Network (HBN) database to assess whether these patterns replicate in a large developmental sample ($N = 224$; age 6–20 years), and whether they relate to reading development. In both datasets, we find that VWFA-1 is primarily correlated with bilateral visual regions. In contrast, VWFA-2 is more strongly correlated with language regions in the frontal and lateral parietal lobes, particularly the bilateral inferior frontal gyrus. Critically, these patterns do not generalize to adjacent face-selective regions, suggesting a specific relationship between VWFA-2 and the frontal language network. No correlations were observed between functional connectivity and reading ability. Together, our findings support the distinction between subregions of the VWFA, and suggest that functional connectivity patterns in the ventral temporal cortex are consistent over a wide range of reading skills.

KEYWORDS
functional connectivity, language, reading, resting-state fMRI, visual cortex, visual word form area

1 | INTRODUCTION

Over two decades of cognitive neuroscience research have repeatedly located a region in the left ventral occipitotemporal cortex (VOTC) that responds selectively to text (for review, see Caffarra et al., 2021). This region, termed "the visual word form area" (VWFA), is consistently activated when words are presented visually. Interestingly, it was also reported that this area is activated in response to non-visual

linguistic stimuli and tasks (Ludersdorfer et al., 2016; Planton et al., 2019; Price & Devlin, 2003; Reich et al., 2011). In the visual domain, there are mixed findings regarding the functional properties of this region, specifically debates center around the degree of selectivity it shows to language content compared with low-level visual features of text (Caffarra et al., 2021; Dehaene & Cohen, 2011; Vogel et al., 2014; Yeatman & White, 2021) or other visual stimuli (Centanni et al., 2017; Hervais-Adelman et al., 2019; Kubota et al., 2019; Song et al., 2012). Recent evidence suggests that these inconsistencies indicate that the VWFA is not a single, uniform, region, but comprises a series of subregions that differ in the level of computation they perform on the textual input (Lerma-Usabiaga et al., 2018; White et al., 2019; Yeatman & White, 2021; Zhan et al., 2023). Specifically, the more posterior patch, VWFA-1, is sensitive to visual letter-shapes and orthographic information, while the more anterior VWFA-2 is sensitive to the language content of the visual text. These subregions were also shown to differ from each other structurally. First, these functional regions co-occur with different cytoarchitectonic areas in the visual cortex (Kubota et al., 2022; Weiner, Barnett, et al., 2017). Second, diffusion magnetic resonance imaging (dMRI) studies have shown they have different profiles of structural connectivity: VWFA-1 is connected via the vertical occipital fasciculus (VOF) to parietal regions involved in visual spatial attention, namely the inferior parietal sulcus (IPS). In contrast, VWFA-2 overlaps with cortical terminations of the posterior and long segments of the arcuate fasciculus (AF), which carry information between the temporal lobe, parietal lobe, and the frontal lobe (Kubota et al., 2022; Lerma-Usabiaga et al., 2018; Weiner & Yeatman, 2020). Together, the emerging evidence suggests that, despite their proximity, these subregions are specialized for different components of the reading process. Here, we ask whether these subregions are also functionally associated with distinct *functional* networks in the brain.

Resting-state functional connectivity is a methodology where the spontaneous fluctuations in the hemodynamic signal are compared between different regions in the brain. Distant regions that show highly correlated signals over time are considered to belong to the same functional network and share a common function (Biswal et al., 1995). Several studies found that at rest, the VWFA is highly correlated with frontal language regions (Koyama et al., 2010; Koyama et al., 2011; Li et al., 2017, 2020), dorsal attention regions, (Vogel et al., 2012) or both (Chen et al., 2019; Wang et al., 2014; Zhou et al., 2015). Importantly, these studies have typically looked at the VWFA as a single region, defined on a template using predefined coordinates or atlases (Chen et al., 2019; Koyama et al., 2010, 2011; Li et al., 2017, 2020; López-Barroso et al., 2020; Schurz et al., 2015; Vogel et al., 2012; Wang et al., 2014; Zhou et al., 2015). It therefore remains unknown whether these connectivity patterns follow a similar division into subregions, and if so, whether this is specific to the reading network or a general principle of high-level visual cortex.

To tackle these questions, we capitalize on two complementary datasets. We first use the Natural Scenes Dataset (NSD) to define VWFA-1 and VWFA-2 at the individual level in high-quality data, and investigate the functional connectivity patterns of each of these individually defined subregions. Considering the evidence regarding the functional profiles of VWFA-1 and VWFA-2, we hypothesize that VWFA-1 will be strongly correlated with visual and attentional regions. In contrast, we expect VWFA-2 to show stronger functional connectivity with language regions, particularly in the left frontal lobe. We then turn to the Healthy Brain Network (HBN) dataset, a large pediatric sample consisting of hundreds of children and adolescents, to test whether (a) these patterns replicate at scale and (b) connectivity strength between the VWFAs and frontal language regions is associated with reading development.

2 | MATERIALS AND METHODS

2.1 | NSD dataset

The NSD (http://naturalscenesdataset.org) consists of 7T functional MRI (fMRI), anatomical MRI, and diffusion MRI data for eight healthy adult participants (six females) who viewed thousands of color images of natural scenes over multiple scanning sessions (see Allen et al. (2022) for a full description of the dataset). Additionally, each subject completed 20 sessions of resting-state scans and six runs of a visual category localizer ("fLoc") (Stigliani et al., 2015). NSD raw scans, minimally preprocessed data, and contrast maps for the functional localizer that were used for region-of-interest (ROI) definition, are all publicly available (https://cvnlab.slite.page/p/M3ZvPmfgU3/General-Information). See Table 1 for acquisition parameters of the resting-state data.

2.2 | Data preprocessing and denoising

Data were minimally preprocessed using temporal resampling to correct for slice time differences, and spatial resampling to correct for

TABLE 1 Acquisition parameters for the two datasets, Natural Scenes Dataset (NSD) and Healthy Brain Network (HBN). Note that HBN data were collected on multiple scanners.

	NSD	HBN
Scanner	7T Siemens Magnetom	3T Siemens TimTrio 3T Siemens Prisma
TR (ms)	1600[a]	800
TE (ms)	22	30
Spatial resolution (mm)	1.8 Isotropic	2.4 Isotropic
Multiband acceleration factor	3	6
Run duration	300 s	300 s
Frames per run	226	375
Runs per subject	20	2
Total scan time	100 min	10 min

[a]Resampled to TR = 1333 ms.
Abbreviations: TR, repetition time; TE, time to echo.

head motion within and across scan sessions, echo-planar imaging (EPI) distortion, and gradient non-linearities (for more details see Allen et al., 2022). We then transformed each functional run to the individual cortical surface using the utility *nsd_mapdata* (https://github.com/cvnlab/nsdcode) and carried out all subsequent analyses on the native surface of each subject. Data denoising and correlation analysis were carried out using Nilearn v0.9.1 (Abraham et al., 2014). Data were denoised using a general linear model with the following confound regressors and their temporal first derivatives, following the procedure described in Yeo et al. (2011): six motion parameters, the white matter signal (averaged within a white matter mask eroded with four iterations), the ventricular signal, and the global signal averaged within a whole-brain mask. We used an eroded white matter mask to minimize partial voluming between white and gray matter and reduce correlations between the white matter signal and the global signal (Parkes et al., 2018; Power et al., 2017). The global signal was included as a confound regressor due to evidence showing it minimizes the dependency between connectivity measures and motion (Ciric et al., 2017). Although global signal regression can potentially increase negative correlations in the data (Saad et al., 2012), it has been shown to improve the specificity of positive correlations and reduce the influence of motion and respiratory artifacts (Murphy & Fox, 2017). Bandpass filtering was applied simultaneously to the signal and the confound regressors using a fifth-order Butterworth filter (0.008–0.1 Hz). Lasly, we handled volumes with excessive motion by first flagging timepoints where the framewise displacement (FD) exceeded 0.25 mm. We then created a binary ("spike") regressor for each flagged timepoint. Runs where more than 10% of timepoints were flagged for motion, or where the mean FD exceeded 0.25 mm, were discarded from analyses. This process resulted in excluding four runs for subj02, three runs for subj03, and nine runs for subj05.

2.3 | Individual ROI definition

As VWFA-2 is typically found only in the left hemisphere (Kubota et al., 2022; Weiner, Barnett, et al., 2017; White et al., 2019, 2023) and the critical comparison concerns VWFA-1 and VWFA-2, we focus our analyses on seed ROIs within the left hemisphere. We defined text-selective ROIs based on fLoc, a visual category localizer (Stigliani et al., 2015), where subjects viewed grayscale images of stimuli of different categories (e.g., text, faces, limbs, objects, and places). Text-selective regions were identified on individual surfaces by comparing activations to text (pronounceable pseudowords) with the average activation to all other stimuli, except for numbers, thresholded at $t > 3$. These contrast maps are included in the NSD data release. These contrast maps usually reveal multiple patches with several distinct activation peaks. To identify VWFA-1 and VWFA-2, we followed the guidelines in White et al. (2023), focusing on patches within and around the left occipitotemporal sulcus (OTS). VWFA-1 was defined as the posterior text-selective patch just anterior and lateral to area hV4, as suggested by Yeatman et al. (2013). Manually labeled retinotopic ROIs were provided in the NSD release. VWFA-2 was defined as the next anterior, text-selective patch, using the same threshold. Activation clusters that overlapped the mid-fusiform sulcus were not included. We next used the same contrast map (text > all stimuli except numbers) to define text-selective activations in the left frontal lobe. These activations were generally found within the left inferior frontal cortex (IFC), specifically centered around the inferior frontal sulcus (IFS) and inferior portion of the precentral sulcus (PCS), and are referred to as IFC-text hereafter. Lastly, for our control analyses using face-selective ROIs, we used the contrast map of faces versus the average activation to all other categories ($t > 3$) to define face-selective regions along the left fusiform gyrus, namely the fusiform face area (FFA)-1 and FFA-2 (Chen et al., 2023). While face-selective regions are typically found in both hemispheres (Chen et al., 2023; Rosenke et al., 2021), here, we focus on the left hemisphere seed ROIs to delineate the functional organization of the left VOTC around the text-selective regions. See Figure 1 for the ROI delineation process and Table S1 for details on ROI size.

2.4 | Seed-based correlation analysis

For each seed ROI, we extracted the mean time series, averaged across all vertices comprising that ROI. We then calculated Pearson's correlation coefficient between the seed timeseries and the timeseries of all other vertices on the cortical surface to generate a correlation map for each hemisphere. *R* values were converted to *z*-values using the Fisher transform to account for the non-normal distribution of correlation coefficients. We repeated this process separately for each run and then averaged the resulting correlation maps across runs, for each seed ROI for each subject. We used paired samples *t*-test to examine the difference between the correlation maps of VWFA-1 and VWFA-2. Next, to examine these correlations at the group level, we transformed each subject's native surface to the fsaverage template space (using *nsd_mapdata* utility) and created group correlation maps across subjects ($N = 8$). This whole-brain analysis provided us with a spatial distribution of the correlation patterns of VWFA-1 and VWFA-2 throughout the brain. All analyses were carried out using Nilearn v0.9.1 and visualized with Freeview v7.3.2 (https://surfer.nmr.mgh.harvard.edu/).

2.5 | ROI-to-ROI correlation analysis

To directly test the hypothesis that VWFA-2 is more strongly connected to specific language regions in the frontal lobe, we ran an ROI-to-ROI analysis where we quantified the connectivity strength between pairs of ROIs. Specifically, we calculate Pearson's correlation coefficient between the timeseries of VWFA-1 and IFC-text, and VWFA-2 and IFC-text.

2.6 | HBN dataset

The HBN database consists of neuroimaging and phenotypic data from over 1500 participants ranging from 5 to 21 years of age from

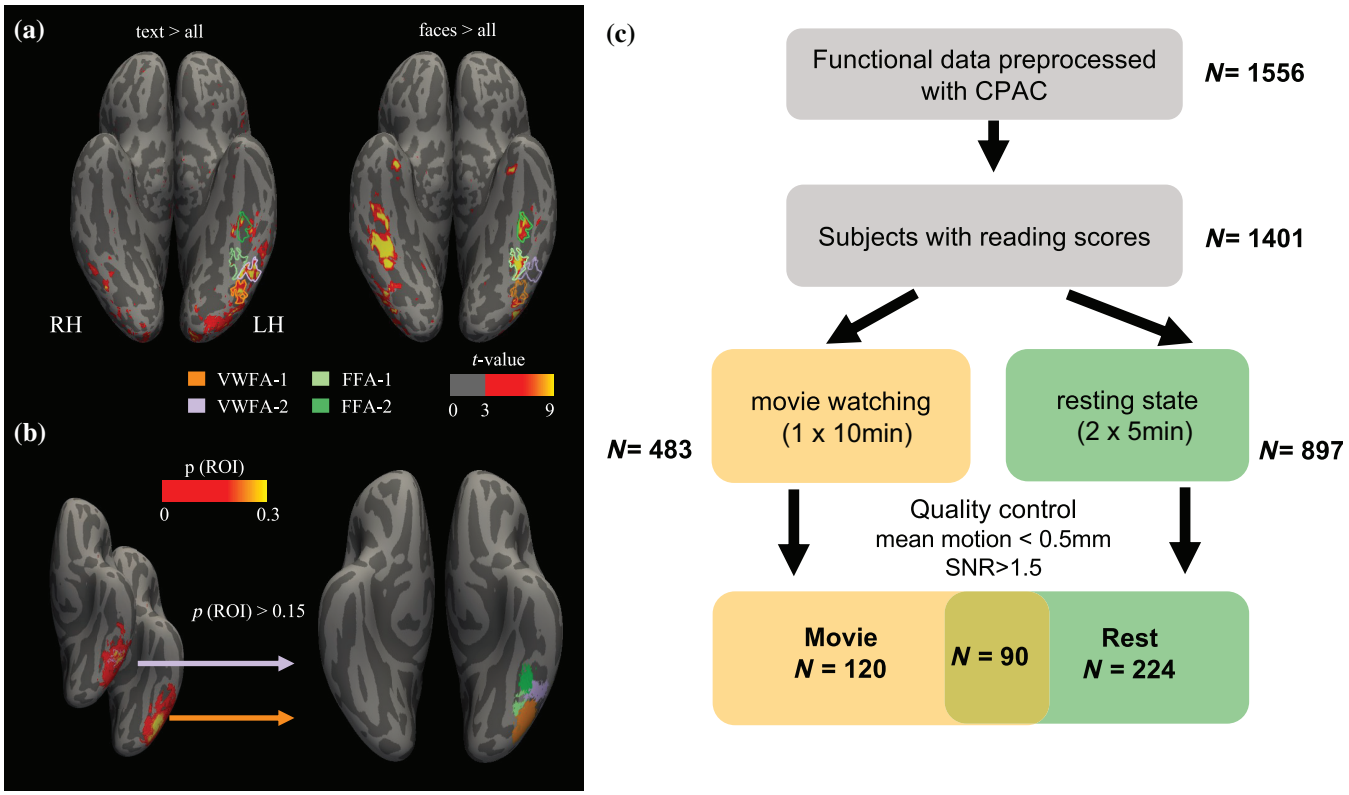

FIGURE 1 (a, b) Definition of category-selective ROIs. (a) For Natural Scenes Dataset (NSD) subjects, the visual word form area (VWFA-1) and VWFA-2 were defined using thresholded maps of text-selective responses (text > all other categories; $t > 3$) on the individual cortical surface. Similarly, FFA-1 and FFA-2 were defined using the contrast faces > all other categories, with the same threshold. (b) Definition of group ROIs used for analysis of Healthy Brain Network (HBN) data. Probabilistic maps were created by transforming individual ROIs defined in an independent sample of 28 adults to the fsaverage template. These maps were thresholded at $p > .15$. The same procedure was used to define both text-selective and face-selective ROIs. (c) Schematic of the sample selection process from the HBN database. LH, left hemisphere; RH, right hemisphere; SNR, signal-to-noise-ratio.

the greater New York City area (Alexander et al., 2017). For the current project, we capitalized on the availability of preprocessed functional MRI data ($N = 1556$; publicly available on s3://fcp-indi/data/Projects/HBN/CPAC_preprocessed_Derivatives/). See Table 1 for acquisition parameters.

2.7 | Participant selection

As expected in large pediatric samples, some scans were of low quality or incomplete. We employed a strict quality control threshold to focus our analyses on high-quality, low-motion data. Specifically, we only included scans where the mean FD was lower than 0.5 mm in each of the functional runs, and the signal-to-noise-ratio was higher than 1.5. Figure 1 describes the full selection process that led to a final sample of $N = 224$ participants who completed two high-quality resting-state runs in addition to reading evaluation. In addition, we analyzed a partially overlapping sample of $N = 120$ participants who completed a single high-quality movie-watching run (equivalent in duration to the two resting-state runs) and reading assessments. Inspection of the distribution revealed that despite the strict selection criteria, the resulting sample spanned children of all ages and a wide range of reading ability (see Table 2). Since this database includes a high proportion of individuals affected by various psychiatric and learning conditions, we did not exclude participants based on their diagnoses. Of the 224 participants, 34 did not have any diagnosis, 44 had a dyslexia diagnosis, and the rest had other conditions (e.g., anxiety and mood disorders).

TABLE 2 Healthy Brain Network (HBN) sample characteristics.

	Rest	Movie
N	224	120
Age (years)	12.5 ± 3.3 (6.4–20.8)	12.4 ± 3.5 (6.3–20.1)
Gender	98 F/126 M	48 F/72 M
WIAT word reading standard score	101 ± 17 (40–144)	101 ± 17 (47–136)
In-scanner motion (mean FD, mm)	0.15 ± 0.04 (0.06–0.31)	0.17 ± 0.06 (0.06–0.34)

Abbreviations: FD, framewise displacement; WIAT, Wechsler Individual Achievement Test.

2.8 | Preprocessing

We obtained fully preprocessed and denoised functional data from the publicly available fcp-indi bucket on Amazon Web Services (s3://fcp-indi/data/Projects/HBN/CPAC_preprocessed_Derivatives). The preprocessing steps had been run using the Configurable Pipeline for the Analysis of Connectomes (CPAC) package (Craddock et al., 2013) and are repeated here for completeness. No additional preprocessing steps were carried out after downloading the data. Standard preprocessing steps began with deobliqing and reorienting the anatomical scan. The functional scans were then motion corrected, skull stripped, and coregistered with the anatomical scan. Data were resamped to $2 \times 2 \times 2$ mm voxel resolution and warped to the Montreal Neurological Institute (MNI) standard space. Denoising included the following regressors: six motion regressors, their quadratic terms, delayed regressors and quadratic delayed regressors; polynomial detrending with linear and quadratic terms. aCompCor was used to remove the first five components of the white matter and cerebrospinal fluid (CSF) components. Bandpass filtering was applied to maintain the frequency range (0.01–0.1 Hz). Volumes with excessive motion (FD >0.5 mm) were flagged for spike regression, in addition to the previous volume and the following two volumes. Lastly, the data were demeaned and normalized such that all signal timeseries are represented as *z*-scores.

2.9 | Template ROI definition

As no visual localizer was available for this dataset, we used template ROIs defined in the standard Freesurfer fsaverage template space. Due to the large variability in size and location of these regions (e.g., Glezer & Riesenhuber, 2013; Rosenke et al., 2021), we sought template ROIs defined in a sample larger than the NSD database. To this end, we used ROIs defined as probability maps on an independent sample of adults ($N = 28$; see Kubota et al. 2022), who completed the same category localizer used by the NSD project (Stigliani et al., 2015). VWFA ROIs were defined by comparing the activations to text with the average activation to all other categories, except for numbers (thresholded at $t > 3$), in the left hemisphere. Then, individual ROIs were transformed to fsaverage space to generate a probabilistic map where each vertex equals 1 if there was a perfect overlap across subjects in that location, or zero if none of the subjects had that ROI in that location (same procedure as in Rosenke et al. 2021). These probability maps were thresholded at 0.15 (see Figure 1). The same procedure was used to define the face-selective ROIs in the left hemisphere, FFA-1 and FFA-2. To avoid confusion with the individual ROIs used for NSD, we refer to these group ROIs as gVWFA-1, gVWFA-2, gFFA-1, and gFFA-2.

We used a more lenient threshold of $t > 2$ to define the frontal text-selective ROI, as text-selective activations were weaker in the left frontal cortex than the left occipitotemporal ROIs, and less consistent in location across individuals. Then, the group ROI probability map was thresholded at 0.15 in the same manner as the ventral ROIs, smoothed with one step and anatomically constrained to the sulcus, to generate the template gIFC-text ROI.

2.10 | Group seed-based correlation analysis

As a first step, all data were transformed from volume to fsaverage surface space using nilearn vol2surf function. We then followed the same procedure described above for the NSD dataset, namely, using gVWFA-1, gVWFA-2, and gIFC-text as seeds for whole-brain correlation analysis. We generated correlation maps where each vertex has the value of the *z*-transformed Pearson's correlation value with the seed ROI timeseries. Statistical analyses were carried out across subjects. Specifically, we used vertex-wise paired sample *t*-tests to examine the difference between the correlation maps of gVWFA-1 and gVWFA-2 across subjects. We present these *t*-test maps thresholded at $p = .01$, Bonferroni corrected for the number of vertices (uncorrected $p = 3e{-}8$).

2.11 | ROI-to-ROI correlation analysis

We followed the same procedure described above for the NSD database, this time using the template ROIs. We calculated Pearson's correlation coefficient between the timeseries of gVWFA-1 and gIFC-text, and gVWFA-2 and gIFC-text. These ROI-to-ROI correlation values were used for the statistical analyses described below.

2.12 | Examining connectivity patterns of face-selective ROIs

To determine whether the effects we found were specific to the reading-related VWFA ROIs or reflect a general functional organization of the ventral cortex, we repeated all the correlation analyses reported above while using face-selective ROIs as seeds, namely gFFA-1 and gFFA-2. We then ran an ROI-to-ROI correlation analysis, calculating the correlations between the timeseries of gFFA-1 and gIFC-text, and gFFA-2 to gIFC-text. We used gIFC-text as a frontal ROI for this analysis since no face-selective activations were identified in the IFC. Lastly, we ran a linear mixed effects model using the lme4 package in R (Bates et al., 2015), to assess how functional connectivity strength between each ventral ROI and IFC-text is influenced by visual category (text vs. faces), location (posterior OTS vs. mid-OTS) and their interaction. We then added to the model age, gender, and participant motion in the scanner (average FD) as additional fixed effects, to examine how these subject specific characteristics interact with functional connectivity strength. All models included random intercepts for each subject. We compared models using the AANOVA function in R to determine which of the factors and interactions made a significant contribution to the model fit.

2.13 | Brain-behavior association

To investigate whether functional connectivity patterns are associated with reading development, we fit ordinary least squares regression models with either reading skill or age as the dependent variable and functional connectivity strength, gender, and participant motion in the scanner (average FD) as predictors. Reading skill was measured using the single word reading subtest of the Wechsler Individual Achievement Test (WIAT). Unless otherwise noted, age standardized scores were used, to tease apart the effects of reading skill from age.

3 | RESULTS

3.1 | VWFA-2 is functionally connected to frontal language regions across individuals

We first evaluated seed-based functional connectivity maps in individual subjects using the NSD database. Both VWFA-1 and VWFA-2 showed correlations with large patches in bilateral ventral occipital cortex and inferior parietal cortex. While VWFA-1 was more strongly correlated with ventral and dorsal visual regions in the occipital, temporal, and parietal lobes, VWFA-2 showed stronger correlations with regions in the frontal lobe, including the PCS, IFS and inferior frontal gyrus (IFG), bilaterally. Figure 2a shows the connectivity maps for a single participant (and see Figures S1–S3 for the entire sample). Strong functional connectivity between VWFA-2 and regions of IFC was clear at the individual level, although the exact location and size varied. To compare the functional connectivity patterns of VWFA-2 and VWFA-1, we next calculated a paired sample *t*-test of the two correlation maps within each subject (Figures 2c and S4–S6). This analysis confirms that VWFA-2 shows significantly stronger correlations with the IFC at the individual level for most participants (six out of eight). While the magnitude and exact location of this effect are variable across participants, unthresholded maps (Figures S4–S6) reveal remarkable consistencies in the general spatial pattern of the VWFA-2/VWFA-1 connectivity comparison across the eight participants. Of note, one of the subjects where the effect was not observed had poor data quality due to substantial motion (9/20 runs were excluded from analyses due to motion, see Section 2 for exclusion criteria).

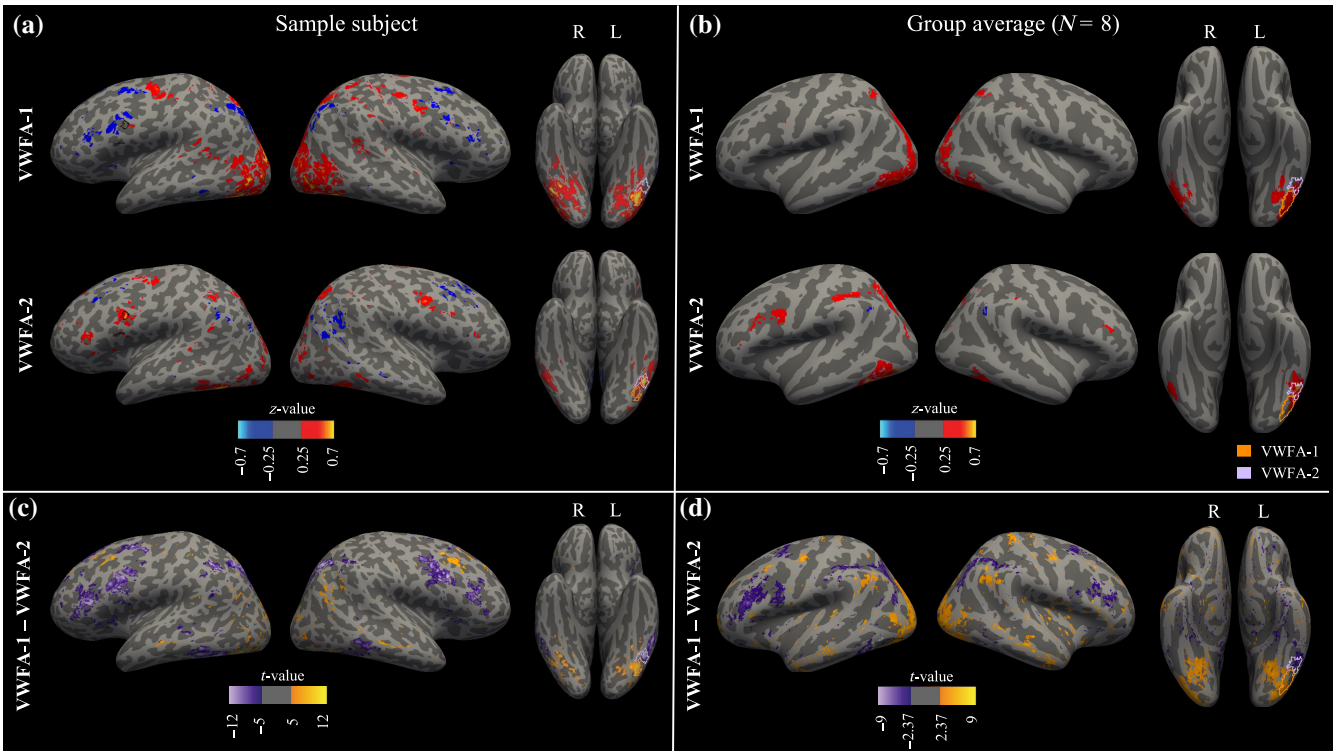

FIGURE 2 Visual word form area (VWFA-1) and VWFA-2 show distinct patterns of functional connectivity at the individual level. (a, b) Seed-based whole-brain functional connectivity maps for VWFA-1 (top row) and VWFA-2 (bottom row) overlaid on inflated cortical surfaces, for a representative subject from the Natural Scenes Dataset (NSD) dataset (subj03; panel a) and averaged across the NSD sample ($N = 8$; panel b). Maps depict Fisher *z*-transformed Pearson correlation coefficients. (c, d) Significant differences in connectivity strength quantified using paired samples *t*-test for subj03 (panel c) and averaged across the sample (d). In both (c) and (d), positive values represent stronger connectivity with VWFA-1, negative values represent stronger connectivity with VWFA-2. Note the different threshold used for within subject analysis ($t > 5$, $p < .0001$, $n = 20$ runs) and group analysis ($t > 2.365$, $p = .05$ uncorrected, $N = 8$ participants). Unthresholded maps of individual subjects reveal the same patterns and are provided in Figures S4–S6. In all panels, seed ROIs are shown on the ventral surface in orange (VWFA-1) and lilac (VWFA-2) contours. See Figures S1–S3, for correlation maps of all individual NSD participants.

To summarize the individual effects observed in NSD data, we transformed the individual correlation maps into fsaverage template space and averaged them across participants. This group analysis revealed a consistent patch spanning the posterior part of the IFG, PCS, and precentral gyrus (PCG), that showed stronger correlations with VWFA-2 compared with VWFA-1 ($p < .05$, uncorrected). Thus, the high-precision, 7T NSD data revealed different patterns of functional connectivity between functionally defined VWFA-1 and VWFA-2 at the individual level, and the template-based group average of these data indicated consistency in this effect across the eight participants.

After establishing that VWFA-2, compared with VWFA-1, is more strongly correlated with IFC in high-quality *adult* data, we turned to the HBN database to determine whether this pattern generalizes at scale in hundreds of individuals, and, importantly, whether it can be observed in a *developmental* population. To this end, we repeated the same seed-based analysis using template-based ROIs and compared the correlation maps of gVWFA-1 and gVWFA-2 across participants in the HBN sample (Figure 3). These maps revealed, again, that despite the similarities between the correlations maps (Table S2), some differences stand out: VWFA-1 is more strongly correlated with regions in the ventral occipital cortex, bilaterally, and inferior parietal regions (see Figure S7), while VWFA-2 is more strongly correlated with frontal regions and lateral parietal regions, primarily in the left hemisphere. These patterns were consistent for resting-state data ($N = 224$) and movie-watching data ($N = 120$).

To quantify the similarity of the group connectivity maps across the two datasets, we calculated the vertex-wise correlation between the group connectivity maps for each seed ROI across datasets. The correlation between maps of the same ROIs in NSD versus HBN data was on average 0.75, compared with 0.56 for different ROIs. This highlights the striking similarity in the observed connectivity patterns across datasets with different characteristics and populations (compare Figure 2b for NSD and Figure 3a for HBN).

3.2 | Text-selective regions in the frontal lobe show stronger functional connectivity with VWFA-2 compared with VWFA-1

We next set out to determine whether the correlations observed between VWFA-2 and the frontal lobe were related to language

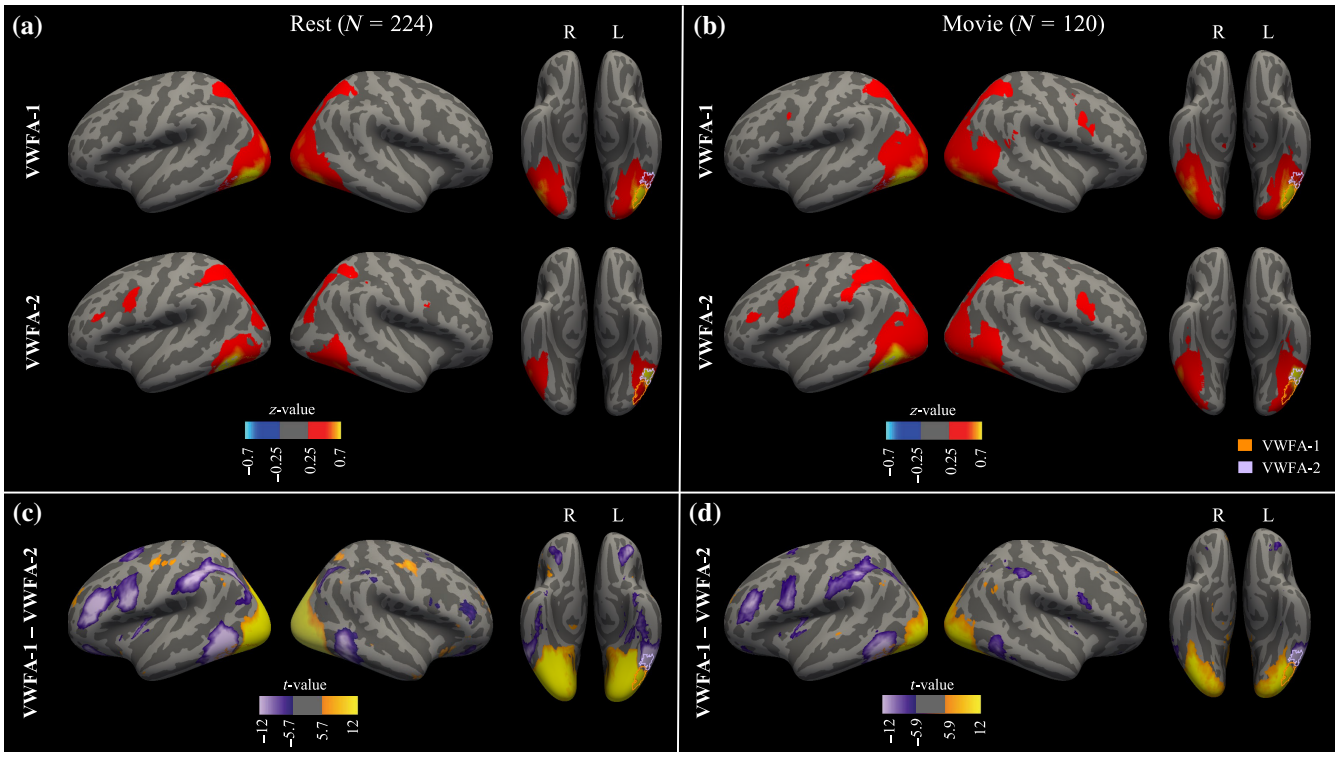

FIGURE 3 Visual word form area (VWFA-1) and VWFA-2 show distinct patterns of functional connectivity in a large group of children and adolescents. (a, b) Seed-based whole-brain functional connectivity maps for VWFA-1 (top row) and VWFA-2 (bottom row) overlaid on inflated cortical surfaces, for resting state (panel a; $N = 224$) and movie watching (panel b; $N = 120$). Maps depict Fisher z-transformed Pearson correlation coefficients. (c, d) Significant differences in connectivity strength quantified using paired samples t-test for resting state (panel c) and movie watching (d) (posterior view shown in Figure S7). In both (c) and (d), positive values represent stronger connectivity with VWFA-1, negative values represent stronger connectivity with VWFA-2. Maps are thresholded at $p = .01$, Bonferroni corrected for the number of vertices (uncorrected $p = 3e{-}8$). In all panels, seed ROIs are shown on the ventral surface in orange (VWFA-1) and lilac (VWFA-2) contours.

function. To this end, we defined a text-selective region in IFC for each NSD participant, and used it as a seed for functional connectivity to inspect how the correlation pattern of that frontal region maps onto the ventral surface. This analysis revealed a striking correspondence between the connectivity map of IFC-text and the boundary between VWFA-1 and VWFA-2, both at the individual level and at the group level across the eight participants (Figure 4).

To quantify this effect, we calculated the average correlation values between IFC-text and each of the two VWFA ROIs (Figure 4b). Functional connectivity between IFC-text and VWFA-2 was stronger compared with VWFA-1 (paired samples $t(7) = 3.85$, $p = .0063$). This finding confirms that VWFA-2 is more strongly correlated than VWFA-1 with text-selective regions in the frontal lobe.

We then repeated the same analyses in the HBN dataset. Critically, as no individual localizer data are available for this dataset, we used template ROIs defined using text-selective activations in an independent dataset (see Section 2). Even when using template ROIs as approximations for text-selective activations, our findings replicated at scale in this pediatric cohort (Figure 5): First, the correlation map of gIFC-text overlaps with gVWFA-2, not gVWFA-1, both for resting-state data and movie-watching data (Figure 5). Second, the ROI-to-ROI analysis confirmed that gIFC-text is more strongly correlated with gVWFA-2 compared with gVWFA-1, both when considering classical resting-state data ($t(223) = 15.39$, $p < 1e{-}36$) and movie-watching data ($t(119) = 12.11$, $p < 1e{-}21$). This shows that the correlation between frontal language regions and VWFA-2 generalizes across populations (adults and children) and tasks (rest and movie watching).

3.3 | Correlations between ventral occipitotemporal cortex and inferior frontal cortex are greater in the reading network

We next set out to determine whether these effects are specific to the reading circuitry, or, alternatively, stem from a general organizational principle of VOTC. For example, we might hypothesize that the differences between VWFA-1 and VWFA-2 functional connectivity represent a general transition in connectivity between posterior and anterior regions of VOTC. To this end, we first overlaid the face-selective ROIs (FFA-1, FFA-2) on the IFC-text connectivity map. We found that while the connectivity "hotspots" overlap VWFA-2, they do not extend medially to the face-selective ROIs (Figure 6). To quantify this effect, we ran an ROI-to-ROI analysis on the resting-state data ($N = 224$), which revealed that FFA-2 has stronger connectivity with IFC-text compared with FFA-1, but it is still significantly weaker than the effect observed for VWFA-2-IFC: The median connectivity between VWFA-2 and IFC-text was 0.46 (95% confidence interval [CI] = [0.41, 0.48]), whereas the median connectivity between FFA-2 and IFC-text was 0.27 (95% CI = [0.24, 0.29]). A linear mixed effect model confirmed that functional connectivity values with the frontal lobe were significantly greater for text-selective regions compared with face-selective regions ($\beta = .028$, $t = 2.28$, $p = .0232$) and for mid-OTS regions compared with posterior OTS regions ($\beta = .053$, $t = 4.274$, $p = 2e{-}5$). Importantly, the interaction between category and location was also highly significant ($\beta = .165$, $t = 9.386$, $p < 2e{-}16$), indicating that the correlation between VWFA-2 and the IFC was significantly stronger compared to the other ventral ROIs. These effects remained the same when participant age, gender, and

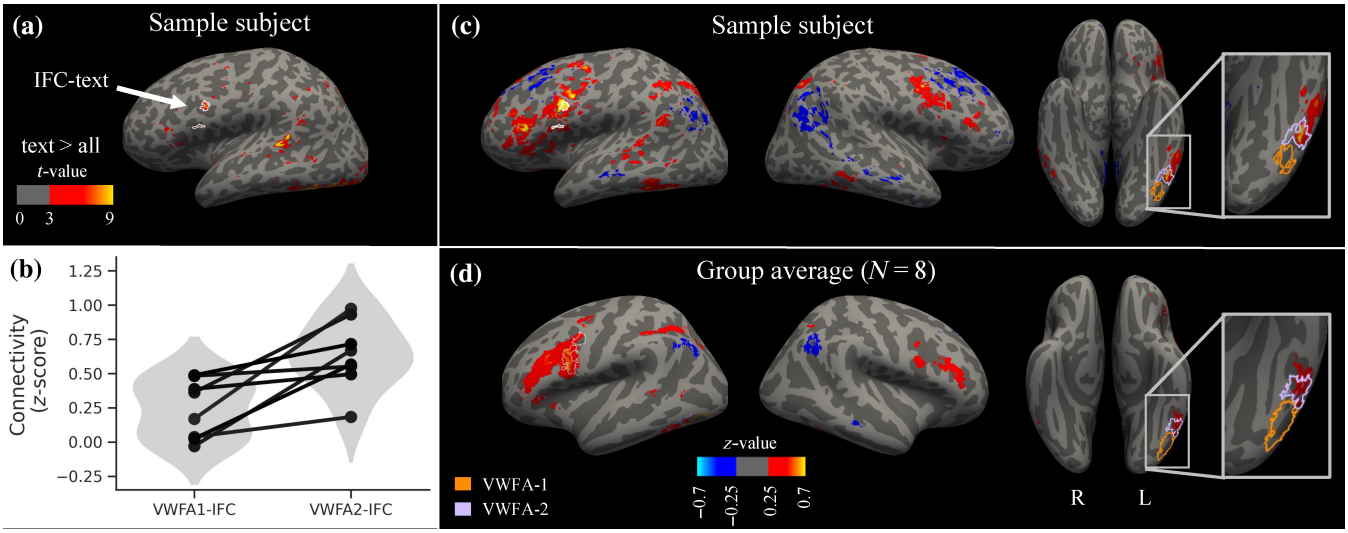

FIGURE 4 Frontal language regions show stronger connectivity with visual word form area (VWFA-2) compared with VWFA-1. (a) Text-selective activations (text vs. all other categories, $t > 3$) for a single subject (subj03). The frontal activation patches selected as the frontal ROI (inferior frontal cortex [IFC]-text) are delineated in white contour. (b) ROI-to-ROI correlation analyses confirmed that the frontal ROI is more strongly connected with VWFA-2, compared to VWFA-1 ($t(7) = 3.85$, $p = .0063$). Each line represents a single participant ($N = 8$). (c, d) Seed-based whole-brain functional connectivity maps for the frontal text-selective region (IFC-text) overlaid on inflated cortical surfaces, for a representative subject (c; subj03) and averaged across the Natural Scenes Dataset sample (d; $N = 8$). Maps depict Fisher z-transformed Pearson correlation coefficients. IFC-text for the participant in panel (c) is delineated by white contour. In panel (d), ROI contours represent template ROIs.

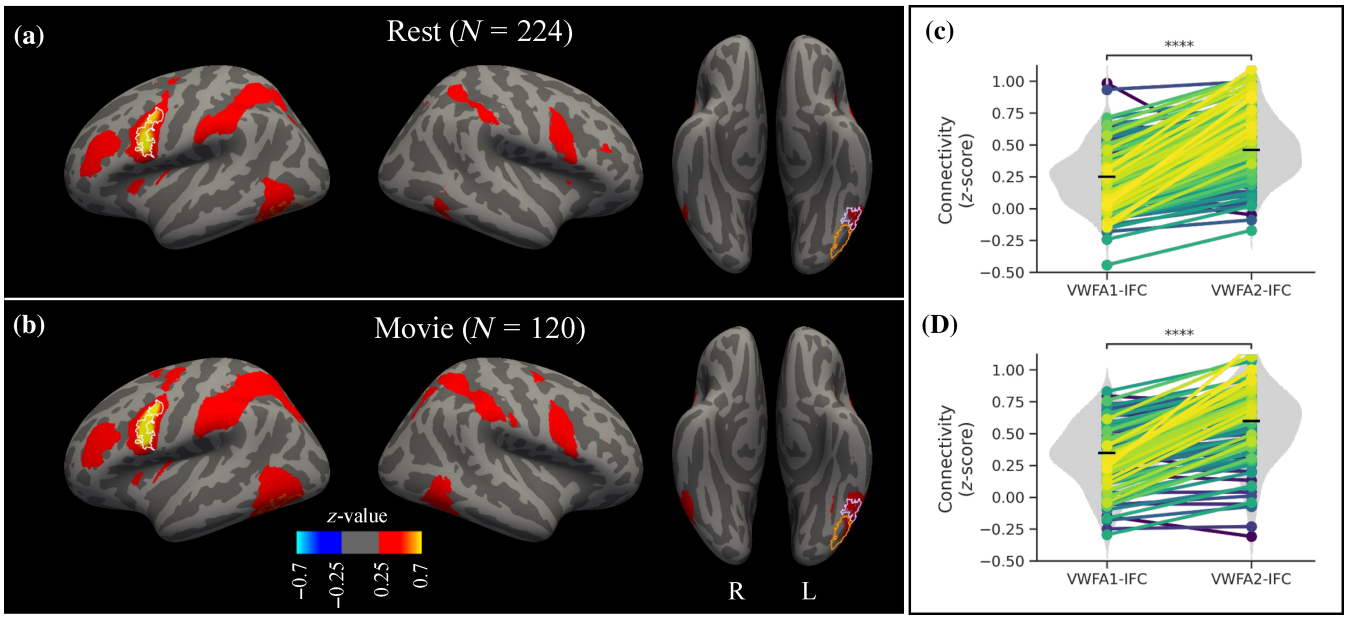

FIGURE 5 Frontal language regions show stronger connectivity with visual word form area (VWFA-2) compared with VWFA-1. (a, b) Seed-based whole-brain functional connectivity maps for the frontal text-selective region (inferior frontal cortex [IFC]-text) overlaid on inflated cortical surfaces, averaged across the HBN sample for resting-state data (a) and movie-watching data (b). Maps depict Fisher *z*-transformed Pearson correlation coefficients. IFC-text is shown in white contour. (c, d) ROI-to-ROI connectivity strength between IFC-text and VWFA subregions. Connectivity is significantly stronger between IFC-text and VWFA-2 compared with VWFA-1 (c: resting state, $t(223) = 15.39$, $p < 1e{-}36$; d: movie watching, $t(119) = 12.11$, $p < 1e{-}21$). Lines are color coded for the magnitude of the difference in connectivity strength between IFC-text and VWFA-1 compared with VWFA-2, with larger differences in lighter colors. Black horizontal lines denote the median. **** p < 1e-20.

motion were included in the model as between subject variables. While age and subject motion each increased functional connectivity values overall (age: $\beta = .011$, $t = 3.035$, $p = .0027$; motion: $\beta = .599$, $t = 2.262$, $p = .0247$), gender was unrelated to functional connectivity strength ($\beta = .008$, $t = 0.321$, $p = .748$). To test whether any of these factors had a specific effect on VWFA2-IFC connectivity strength, we ran three separate models that included the three-way interaction between category, location, and each of the variables of interest (age, gender, and motion), and compared them to the baseline model that included only the main effects. None of the three-way interactions nor the two-way interactions with age, gender, or motion were significant. An analysis of variance (ANOVA) comparing the models revealed that including these interactions did not improve the model fit beyond the contribution of the main effects of these variables. Running the same analysis on the movie-watching data ($N = 120$) revealed comparable effects (category: $\beta = .052$, $t = 2.934$, $p = .0035$; location: $\beta = .039$, $t = 2.181$, $p = .0298$) and a significant interaction showing that the correlation between IFC and VWFA-2 was significantly stronger compared with the other ventral ROIs ($\beta = .184$, $t = 7.355$, $p = 1e{-}12$). Age, gender, or motion did not make a significant contribution to the model in explaining functional connectivity values in the movie-watching data (all $p > .05$). In sum, this analysis showed that the IFC was more strongly correlated with VWFA-2 compared with the rest of the ventral ROIs, above and beyond the effect of location along the posterior–anterior axis. This effect is independent of subject age, gender, and motion.

To further explore the spatial distribution of the correlations of the face-selective compared to text-selective regions, we repeated our primary functional connectivity analysis using the face-selective ROIs as seeds. The resulting maps revealed that the correlations between FFA-1 and FFA-2 and IFC were significantly weaker than the correlation observed between VWFA2- and IFC-text (Figures 7 and S8): Using the same threshold, no patches of functional connectivity were observed in the frontal lobe. To quantify the similarity between the text- and face-selective connectivity patterns, we calculated the vertex-wise correlations across the group mean connectivity maps for each seed ROI. We found that the VWFA-1 connectivity map was more similar to the map of FFA-1 ($r = 0.957$) than it was to VWFA-2 ($r = 0.729$; see Table S2). Lastly, we compared the whole-brain correlation maps of VWFA-2 to those of FFA-2 to see how they differ spatially throughout the brain (Figure 7c,d). This revealed that VWFA-2 is more strongly correlated than FFA-2 with two large patches in the frontal lobe, as well as with a large area in the lateral parietal lobe. In contrast, FFA-2 is more strongly correlated with regions in the superior temporal sulcus and the central sulcus.

3.4 | VWFA functional connectivity is associated with age, but not with reading ability

We next examined whether the functional connectivity strength between VWFA-1/2 and the frontal ROI is associated with reading

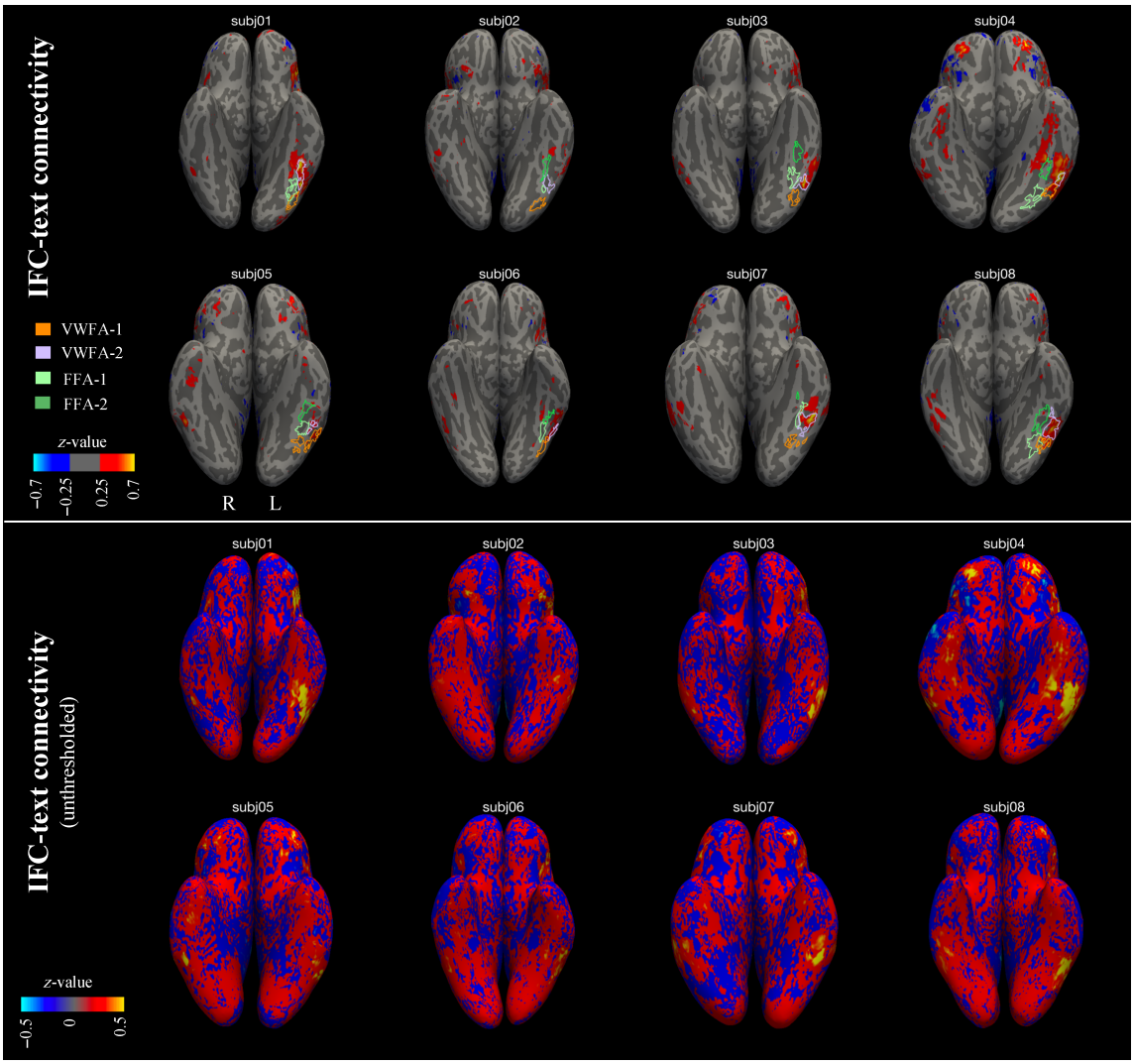

FIGURE 6 IFC-text is specifically correlated with VWFA-2. Shown are functional connectivity maps for the text-selective frontal ROI (IFC-text) on the ventral surface of individual subjects. Top panel: thresholded correlation maps with contours of individually defined category-selective ROIs. Bottom panel: unthresholded correlation maps.

development. We first used an ordinary least squares regression model, with age as the dependent variable, and functional connectivity values (VWFA-1 to IFC-text and VWFA-2 to IFC-text), gender, and average head motion (mean FD averaged across runs) as predictors. This model allowed us to evaluate the relationship between functional connectivity and age, above and beyond the contribution of motion and gender. We found that functional connectivity strength between VWFA-1 and IFC-text was a significant predictor of age ($\beta = 4.080$, $p = .0009$), such that the correlation between VWFA-1 and the frontal language region increased with age. As expected, motion was highly predictive of age ($\beta = -19.426$, $p = .00003$), as younger children tend to move more in the scanner. In total, the model explained 11% of the variance in age ($F = 7.153$, $p = .00002$). We next created a second model predicting reading ability, which was operationalized as the age standardized single word reading subtest from the WIAT battery. We included the same predictors as in the previous analysis. The only significant predictor of reading skill was motion ($\beta = -71.629$, $p = .0068$), but the full model failed to reach significance and explained less than 5% of the variance in reading ability. In line with these results, the simple correlation between age and functional connectivity strength between IFC and VWFA-1 was significant ($r = 0.206$, $p = .002$; see Figure 8), while the other simple correlations between connectivity values and age or reading were non-significant (all $p > .05$). Applying the same regression models to the movie-watching data did not reveal any significant effects except for the association between motion and age ($\beta = -2.85$, $p = .007$).

4 | DISCUSSION

We found, in two independent datasets, that subregions of the VWFA show distinct patterns of functional coupling at rest with distant brain regions: The more posterior VWFA-1 is strongly correlated with visual and attentional regions in the occipital and parietal cortex, while the

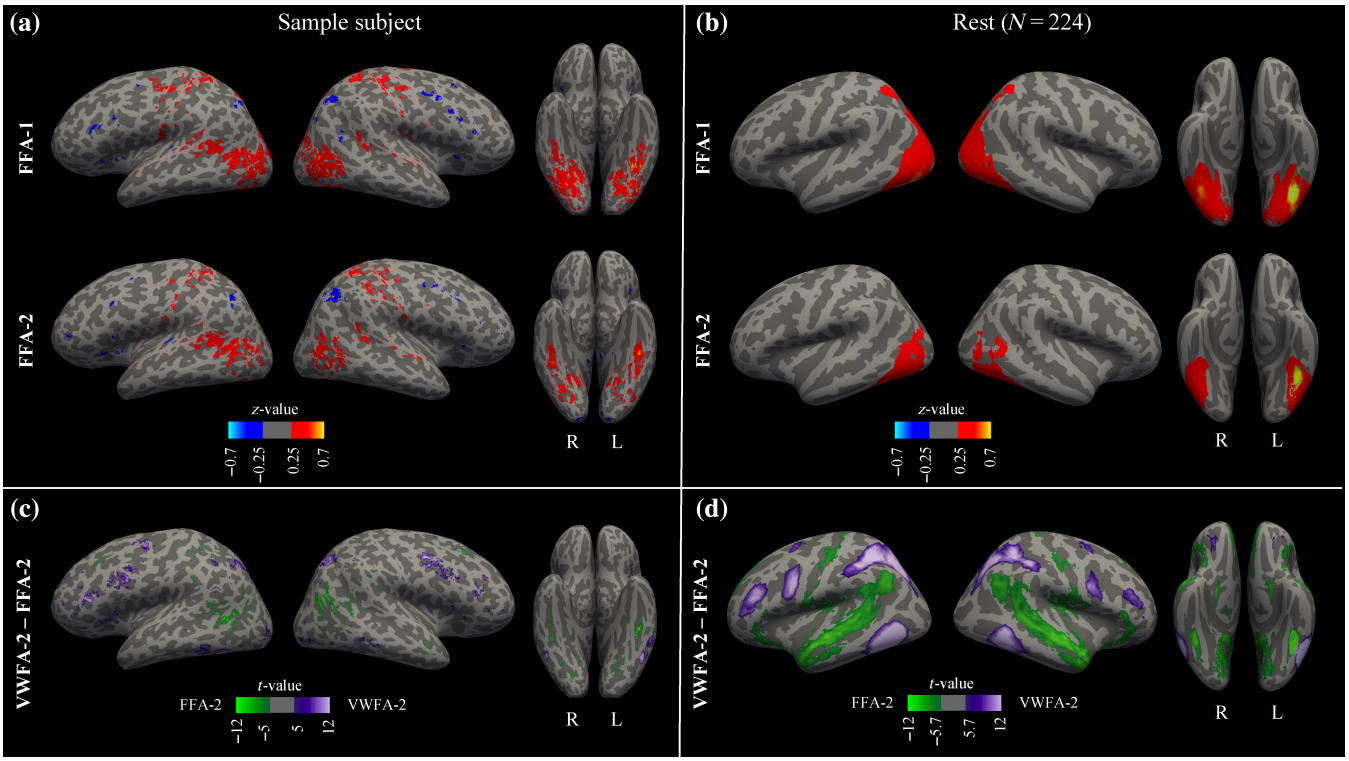

FIGURE 7 Face-selective ROIs do not show the same connectivity patterns with the frontal lobe as the text-selective ROIs. (a, b) Seed-based whole-brain functional connectivity maps for the face-selective ROIs, FFA-1 and FFA-2 overlaid on inflated cortical surfaces, for a single subject from the Natural Scenes Dataset (subj03; a) and averaged across subjects from the Healthy Brain Network (HBN) dataset (b). Maps depict Fisher *z*-transformed Pearson correlation coefficients. (c, d) *t*-Test maps showing the difference in connectivity values between VWFA-2 and FFA-2, for the same single subject (c) and averaged across the HBN sample (d). Note the different threshold used for within subject analysis ($t > 5$, $p < .0001$, $n = 20$ runs, as in Figure 2c) and group analysis ($p = .01$, Bonferroni corrected for the number of vertices (uncorrected $p = 3e{-}8$), $n = 224$ subjects, as in Figure 3c).

more anterior VWFA-2 is strongly correlated with language regions in the frontal lobe. We established this distinction first at the individual level in high-quality adult data using individually defined ROIs. We then confirmed that these patterns replicate at scale in a large sample of children and adolescents, and found that they are unrelated to reading ability. Importantly, we show that these patterns manifest in the reading circuitry yet do not generalize to adjacent face-selective ROIs.

These findings are in line with the structural connectivity literature detailing the white matter connections of the VWFA (Bouhali et al., 2014; Lerma-Usabiaga et al., 2018; Yeatman et al., 2013). Recent studies reported that posterior and mid/anterior portions of the VTC are connected to different brain areas via separate long-range white matter pathways. Specifically, posterior regions were shown to be connected to the inferior parietal lobe through the VOF (Weiner, Yeatman, & Wandell, 2017; Yeatman et al., 2014). In contrast, more anterior portions of the VTC were shown to connect with frontotemporal regions through the AF, a large tract spanning the temporal, parietal, and frontal lobes, that has been repeatedly associated with reading and language abilities (Broce et al., 2015; Gullick & Booth, 2015; Saygin et al., 2013; Skeide et al., 2016; Vandermosten et al., 2012; Yeatman et al., 2011; Yeatman, Dougherty, Ben-Shachar, & Wandell, 2012; Yeatman, Dougherty, Myall, et al., 2012). Recent studies that combined a functional definition of the VWFAs, with dMRI-based fiber tractography, confirmed that functionally defined VWFA-1 and VWFA-2 overlap with endpoints of the VOF and the AF, respectively (Kubota et al., 2022; Lerma-Usabiaga et al., 2018). Our current findings corroborate this distinction, and reveal a correspondence between the functional and the structural connectivity of these adjacent subregions.

In light of these findings, we interpret our results as attesting to the different levels of analysis that are carried out in each subregion of the VWFA. Several studies have reported a hierarchy in the VTC, where sensitivity to lexical features and abstract language information increases along the posterior–anterior axis (Binder et al., 2006; Olulade et al., 2015; Taylor et al., 2019; van der Mark et al., 2009; Vinckier et al., 2007; Zhan et al., 2023). Interestingly, a recent review found that studies that compare responses to text with responses to non-text stimuli, typically reveal text-selective activations in a wide range of locations along the posterior–anterior axis. In contrast, studies that localize the VWFA using lexical contrasts (e.g., comparing real words and pseudowords) consistently report a single, more anterior region (Caffarra et al., 2021). Indeed, when lexical contrasts were directly compared with orthographic contrasts in the same sample,

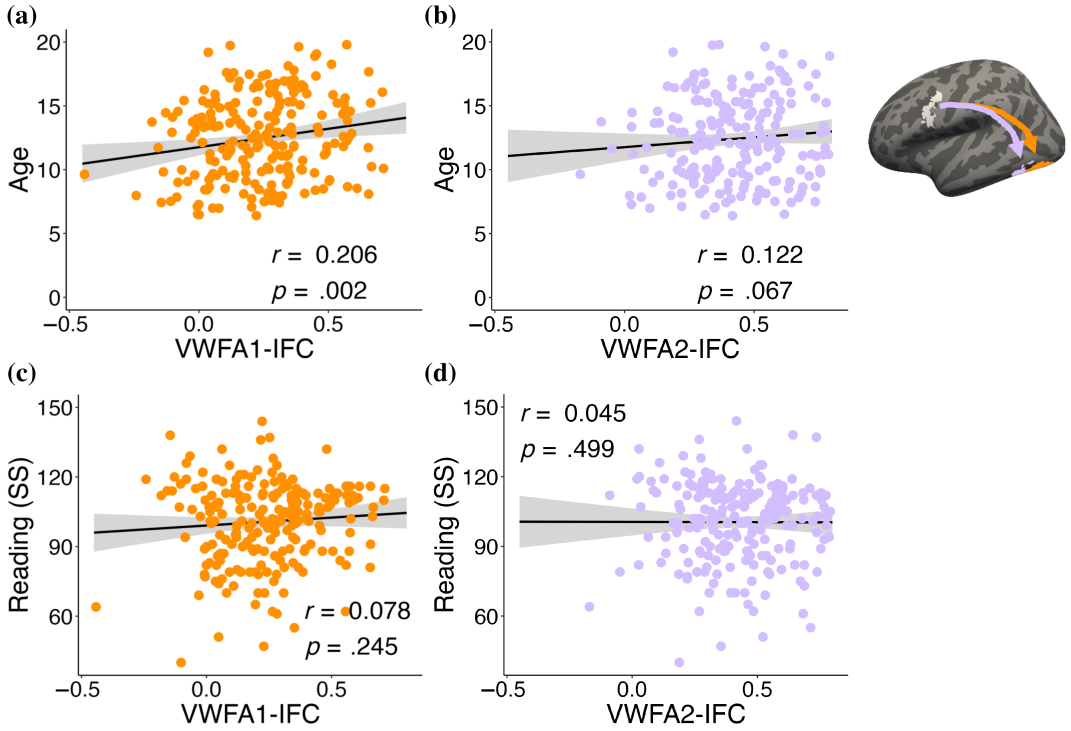

FIGURE 8 Functional connectivity strength is correlated with age, but not with reading ability. The ROIs are shown in the inset, with gVWFA-1 in orange, gVWFA-2 in lilac and the frontal language ROI (gIFC-text) in white. IFC, inferior frontal cortex; SS, standard scores; VWFA, visual word form area.

orthographic contrasts revealed two patches, posterior and anterior, while lexical contrasts resulted in a single anterior patch (VWFA-2) (Lerma-Usabiaga et al., 2018). In addition, VWFA-1 and VWFA-2 were shown to have different response profiles when multiple words are presented in parallel, leading to the suggestion that VWFA-2 serves as a bottleneck for word processing (White et al., 2019). Taken together, the evidence suggests that VWFA-1 processes visual and orthographic information, which then undergoes further processing and integration with the language system in VWFA-2. This distinction in function is supported by our current findings that show that these regions also have differential functional connectivity patterns.

A crucial question is whether these distinct connectivity patterns are specific to the reading network. An alternative explanation would be that this transition in connectivity patterns is an organizational principle of the VOTC, that is independent of category-selectivity. For example, the motif of repeating, category-selective patches has been shown to be a general organizational principle of high-level visual cortex (Freiwald, 2020; Grill-Spector & Weiner, 2014; Tsao et al., 2008; Yeatman & White, 2021). In other words, it could be that there is a general posterior–anterior gradient of connectivity such that more anterior regions have stronger correlations with the frontal lobe. Instead, our findings favor a view of the VWFA-2 as a region with specific connectivity to language regions in the IFC: By examining the connectivity patterns of face-selective ROIs we confirm that (a) VWFA-2 is strongly correlated with IFC-text above and beyond the effects of category-selectivity and location along the posterior–anterior axis. (b) Functional connectivity patterns of frontal text-selective regions within the IFC show a correlation peak that almost perfectly localizes VWFA-2, and does not extend medially to face-selective ROIs (Figure 6). We conclude that there is a unique relationship between VWFA-2 and language regions in the frontal lobe, further supporting its role in bridging visual-orthographic analysis and high-level language processing.

Our findings shed light on inconsistencies in past findings about resting-state functional connectivity of the VWFA. While some studies reported that the VWFA is primarily correlated with frontal language regions (Koyama et al., 2010, 2011; Li et al., 2017; Li et al., 2020; Stevens et al., 2017), others have also found substantial correlations with dorsal attention regions in the parietal lobe (Chen et al., 2019; Wang et al., 2014; Zhou et al., 2015). The correlations with the dorsal attention network were taken to imply that the VWFA serves as a hub for visual attention that is not specific to reading (Vogel et al., 2012). Importantly, past studies have typically looked at the VWFA as a single, uniform region (Chen et al., 2019; Koyama et al., 2010, 2011; Li et al., 2017, 2020; López-Barroso et al., 2020; Schurz et al., 2015; Vogel et al., 2012; Wang et al., 2014; Zhou et al., 2015). Our approach of breaking down the VWFA into subregions reconciles these discrepancies, by uncovering the different connectivity patterns of VWFA-1 and VWFA-2. Future work is warranted to explore further the relationship between these subregions and specific functional networks throughout the brain (e.g., Yeo et al., 2011; see Figure S9).

Several studies reported that reading ability was associated with functional connectivity strength during language tasks (Boets

et al., 2013; Smith et al., 2018; van der Mark et al., 2011; Wise Younger et al., 2017). Critically, task-based functional connectivity may be enhanced or modulated by task demands (White et al., 2023), while resting-state functional connectivity is thought to capture an intrinsic network architecture. Interestingly, evidence linking reading skill to resting-state functional connectivity has been mixed. Several studies reported correlations between functional connectivity strength and reading performance in children (Alcauter et al., 2017; Cross et al., 2021) and adults (Achal et al., 2016; Koyama et al., 2011; Li et al., 2017; López-Barroso et al., 2020; Stevens et al., 2017). However, these associations were found in inconsistent locations throughout the brain, for example, the striatum, thalamus, and frontal lobe. In studies that focused on the VWFA, reading was correlated with functional connectivity strength between the VWFA and either temporal regions (Stevens et al., 2017), or frontal language regions (Koyama et al., 2011; Li et al., 2017). Importantly, correlations with reading were observed in adults but did not generalize to children (Koyama et al., 2011; Li et al., 2017). In our current sample of 224 children, we did not find evidence for correlations between reading ability and functional connectivity of the VWFA. This is in line with a recent large-scale study ($N = 313$) that found that while structural connectivity between the VWFA and language regions predicted reading, functional connectivity between the same regions did not (Chen et al., 2019). Considering past evidence and our current findings, we postulate that the patterns of VWFA functional connectivity may reflect an intrinsic, stable property of the brain. This idea should be examined in future studies employing longitudinal methodologies.

It has been suggested that brain connectivity serves as a blueprint for the organization of category-selective regions (Hannagan et al., 2015). This idea was put forward by observations that category-selective regions in the VTC show specific connections with distant brain regions that are involved in the processing of the same category (Stevens et al., 2015). Longitudinal studies revealed that structural connectivity patterns were observed before the emergence of category selectivity itself (Saygin et al., 2012, 2016). Recent studies have discovered that specific functional connectivity patterns of category-selective regions are already in place in neonates (Kamps et al., 2020; Li et al., 2020). Specifically, Li et al. (2020) found that the general anatomical location of the VWFA (on a template brain) is functionally coupled with the language network in infants. These findings support the view that this cortical region is prewired for language. Our current findings lend further support to this notion by showing that subregions of the VWFA have distinct functional connections with distant regions that correspond to their respective role in word processing. Specifically, our findings reveal a strong connection between frontal language regions and VWFA-2, which does not extend to the adjacent face-selective regions nor to VWFA-1. At the same time, VWFA-1 shows strong connections with visual and attentional regions in the inferior parietal cortex, which are similar to those of the face-selective FFA-1 (Figure S7). This may indicate that in posterior VOTC, functional connectivity is indifferent to category selectivity, while in the more anterior regions, specific connections with distant higher-order regions become more dominant. Together, these findings portray a picture of interacting principles governing the functional organization of VOTC. Importantly, the high-quality individual NSD data revealed that the transition in functional connectivity seems to overlap with the functional distinction of individually defined VWFA-1 and VWFA-2. We therefore postulate that the intrinsic link between frontal language regions and the occipitotemporal cortex may govern the emergence of VWFA-2. Future studies employing causal methodologies (e.g., interventions and longitudinal designs) will be needed to test this hypothesis, and delineate the concurrent developmental trajectory of category-selectivity, functional connectivity, and structural connectivity.

Several limitations of the current study should be acknowledged. Since we capitalized on existing databases, we were not in full control of the experimental paradigms employed. The category localizer collected in NSD allowed us to define VWFA-1 and VWFA-2 using the same contrast (text > not text), without further nuance into their differential response to lexical properties. While this approach had been used to consistently locate two text-selective patches (Kubota et al., 2022; Weiner, Barnett, et al., 2017; White et al., 2019, 2023), future studies should incorporate a more sensitive localizer in order to tease apart the lexical from the visual-orthographic components of VWFA response (as in Lerma-Usabiaga et al., 2018). As for HBN data, no individual localizers were collected and we were limited to using template ROIs for our analyses. While template ROIs might blur individual differences, we were still able to observe a strong differentiation between VWFA-1 and VWFA-2 connectivity patterns and an overlap with IFC-text connectivity. Studies that measure individual text-selective responses in children will help refine these observations and examine whether functional connectivity of individually defined subregions are related to reading ability. Individually identifying retinotopically organized regions involved in attention (e.g., IPS-0; Silver & Kastner, 2009; Wang et al., 2015) is also important to follow up on the distinction between VWFA-1/2 connectivity with dorsal stream visual regions. Lastly, HBN is a psychiatric cohort where the vast majority of participants have a diagnosed psychiatric or neurodevelopmental condition. Despite the high individual variability, we were able to observe clear patterns of functional connectivity both for classical resting state and movie-watching data. However, we cannot rule out that the diversity of this sample obscures a relationship between functional connectivity and reading skill.

ACKNOWLEDGEMENTS

We thank Kendrick Kay for helpful discussions about data processing and analysis. This work was supported by NICHD R01-HD095861 to Jason D. Yeatman, Stanford Maternal and Child Health Research Institute award to Iliana I. Karipidis, the National Science Foundation Graduate Research Fellowship (DGE-1656518) to Emily Kubota, and the Zuckerman-CHE STEM Leadership Program to Maya Yablonski.

CONFLICT OF INTEREST STATEMENT

The authors declare no competing financial interests.

DATA AVAILABILITY STATEMENT

All data reported in this manuscript were obtained from public resources: The Natural Scenes Dataset (NSD; http://naturalscenesdataset.org) and the Healthy Brain Network dataset (HBN; http://fcon_1000.projects.nitrc.org/indi/cmi_healthy_brain_network/index.html).

ORCID

Maya Yablonski https://orcid.org/0000-0002-4432-5275

REFERENCES

Abraham, A., Pedregosa, F., Eickenberg, M., Gervais, P., Mueller, A., Kossaifi, J., Gramfort, A., Thirion, B., & Varoquaux, G. (2014). Machine learning for neuroimaging with scikit-learn. *Frontiers in Neuroinformatics*, *8*, 14.

Achal, S., Hoeft, F., & Bray, S. (2016). Individual differences in adult reading are associated with left temporo-parietal to dorsal striatal functional connectivity. *Cerebral Cortex*, *26*, 4069–4081.

Alcauter, S., García-Mondragón, L., Gracia-Tabuenca, Z., Moreno, M. B., Ortiz, J. J., & Barrios, F. A. (2017). Resting state functional connectivity of the anterior striatum and prefrontal cortex predicts reading performance in school-age children. *Brain and Language*, *174*, 94–102.

Alexander, L. M., Escalera, J., Ai, L., Andreotti, C., Febre, K., Mangone, A., Vega-Potler, N., Langer, N., Alexander, A., Kovacs, M., Litke, S., O'Hagan, B., Andersen, J., Bronstein, B., Bui, A., Bushey, M., Butler, H., Castagna, V., Camacho, N., … Milham, M. P. (2017). Data descriptor: An open resource for transdiagnostic research in pediatric mental health and learning disorders. *Scientific Data*, *4*, 1–26.

Allen, E. J., St-Yves, G., Wu, Y., Breedlove, J. L., Prince, J. S., Dowdle, L. T., Nau, M., Caron, B., Pestilli, F., Charest, I., Hutchinson, J. B., Naselaris, T., & Kay, K. (2022). A massive 7T fMRI dataset to bridge cognitive neuroscience and artificial intelligence. *Nature Neuroscience*, *25*, 116–126.

Bates, D., Mächler, M., Bolker, B., & Walker, S. (2015). Fitting linear mixed-effects models using lme4. *Journal of Statistical Software*, *67*, 1–48.

Binder, J. R., Medler, D. A., Westbury, C. F., Liebenthal, E., & Buchanan, L. (2006). Tuning of the human left fusiform gyrus to sublexical orthographic structure. *NeuroImage*, *33*, 739–748.

Biswal, B., Zerrin Yetkin, F., Haughton, V. M., & Hyde, J. S. (1995). Functional connectivity in the motor cortex of resting human brain using echo-planar MRI. *Magnetic Resonance in Medicine*, *34*, 537–541.

Boets, B., Op de Beeck, H. P., Vandermosten, M., Scott, S. K., Gillebert, C. R., Mantini, D., Bulthe, J., Sunaert, S., Wouters, J., & Ghesquiere, P. (2013). Intact but less accessible phonetic representations in adults with dyslexia. *Science*, *342*, 1251–1254.

Bouhali, F., Thiebaut de Schotten, M., Pinel, P., Poupon, C., Mangin, J.-F., Dehaene, S., & Cohen, L. (2014). Anatomical connections of the visual word form area. *Journal of Neuroscience*, *34*, 15402–15414.

Broce, I., Bernal, B., Altman, N., Tremblay, P., & Dick, A. S. (2015). Fiber tracking of the frontal aslant tract and subcomponents of the arcuate fasciculus in 5–8-year-olds: Relation to speech and language function. *Brain and Language*, *149*, 66–76.

Caffarra, S., Karipidis, I. I., Yablonski, M., & Yeatman, J. D. (2021). Anatomy and physiology of word-selective visual cortex: From visual features to lexical processing. *Brain Structure & Function*, *226*, 3051–3065.

Centanni, T. M., King, L. W., Eddy, M. D., Whitfield-Gabrieli, S., & Gabrieli, J. D. E. (2017). Development of sensitivity versus specificity for print in the visual word form area. *Brain and Language*, *170*, 62–70.

Chen, L., Wassermann, D., Abrams, D. A., Kochalka, J., Gallardo-Diez, G., & Menon, V. (2019). The visual word form area (VWFA) is part of both language and attention circuitry. *Nature Communications*, *10*, 1–12.

Chen, X., Liu, X., Parker, B. J., Zhen, Z., & Weiner, K. S. (2023). Functionally and structurally distinct fusiform face area(s) in over 1000 participants. *NeuroImage*, *265*, 119765.

Ciric, R., Wolf, D. H., Power, J. D., Roalf, D. R., Baum, G. L., Ruparel, K., Shinohara, R. T., Elliott, M. A., Eickhoff, S. B., Davatzikos, C., Gur, R. C., Gur, R. E., Bassett, D. S., & Satterthwaite, T. D. (2017). Benchmarking of participant-level confound regression strategies for the control of motion artifact in studies of functional connectivity. *Neuroimage*, *154*, 174–187.

Craddock, C., Sikka, S., Cheung, B., Khanuja, R., Ghosh, S., Yan, C., Li, Q., Lurie, D., Vogelstein, J., Burns, R., Colcombe, S., Mennes, M., Kelly, C., Di Martino, A., Castellanos, F., & Milham, M. (2013). Towards automated analysis of connectomes: The configurable pipeline for the analysis of connectomes (C-PAC). *Frontiers in Neuroinformatics*, *42*, 10–3389.

Cross, A. M., Ramdajal, R., Peters, L., Vandermeer, M. R. J., Hayden, E. P., Frijters, J. C., Steinbach, K. A., Lovett, M. W., Archibald, L. M. D., & Joanisse, M. F. (2021). Resting-state functional connectivity and reading subskills in children. *NeuroImage*, *243*, 118529.

Dehaene, S., & Cohen, L. (2011). The unique role of the visual word form area in reading. *Trends in Cognitive Sciences*, *15*, 254–262.

Freiwald, W. A. (2020). The neural mechanisms of face processing: Cells, areas, networks, and models. *Current Opinion in Neurobiology*, *60*, 184–191.

Glezer, L. S., & Riesenhuber, M. (2013). Individual variability in location impacts orthographic selectivity in the "visual word form area". *Journal of Neuroscience*, *33*, 11221–11226.

Grill-Spector, K., & Weiner, K. S. (2014). The functional architecture of the ventral temporal cortex and its role in categorization. *Nature Reviews. Neuroscience*, *15*, 536–548.

Gullick, M. M., & Booth, J. R. (2015). The direct segment of the arcuate fasciculus is predictive of longitudinal reading change. *Developmental Cognitive Neuroscience*, *13*, 68–74.

Hannagan, T., Amedi, A., Cohen, L., Dehaene-Lambertz, G., & Dehaene, S. (2015). Origins of the specialization for letters and numbers in ventral occipitotemporal cortex. *Trends in Cognitive Sciences*, *19*, 374–382.

Hervais-Adelman, A., Kumar, U., Mishra, R. K., Tripathi, V. N., Guleria, A., Singh, J. P., Eisner, F., & Huettig, F. (2019). Learning to read recycles visual cortical networks without destruction. *Science Advances*, *5*, eaax0262.

Kamps, F. S., Hendrix, C. L., Brennan, P. A., & Dilks, D. D. (2020). Connectivity at the origins of domain specificity in the cortical face and place networks. *Proceedings of the National Academy of Sciences of the United States of America*, *117*, 6163–6169.

Koyama, M. S., Kelly, C., Shehzad, Z., Penesetti, D., Castellanos, F. X., & Milham, M. P. (2010). Reading networks at rest. *Cerebral Cortex*, *20*, 2549–2559.

Koyama, M. S., Martino, A. D., Zuo, X.-N., Kelly, C., Mennes, M., Jutagir, D. R., Castellanos, F. X., & Milham, M. P. (2011). Resting-state functional connectivity indexes reading competence in children and adults. *The Journal of Neuroscience*, *31*, 8617–8624.

Kubota, E., Grotheer, M., Finzi, D., Natu, V. S., Gomez, J., & Grill-Spector, K. (2022). White matter connections of high-level visual areas predict cytoarchitecture better than category-selectivity in childhood, but not adulthood. *Cerebral Cortex*, *33*(6), 2485–2506.

Kubota, E. C., Joo, S. J., Huber, E., & Yeatman, J. D. (2019). Word selectivity in high-level visual cortex and reading skill. *Developmental Cognitive Neuroscience*, *36*, 100593.

Lerma-Usabiaga, G., Carreiras, M., & Paz-Alonso, P. M. (2018). Converging evidence for functional and structural segregation within the left ventral occipitotemporal cortex in reading. *Proceedings of the National Academy of Sciences of the United States of America*, *115*, E9981–E9990.

Li, J., Osher, D. E., Hansen, H. A., & Saygin, Z. M. (2020). Innate connectivity patterns drive the development of the visual word form area. *Scientific Reports*, *10*, 18039.

Li, Y., Zhang, L., Xia, Z., Yang, J., Shu, H., & Li, P. (2017). The relationship between intrinsic couplings of the visual word form area with spoken

language network and reading ability in children and adults. *Frontiers in Human Neuroscience*, *11*, 237.

López-Barroso, D., Thiebaut de Schotten, M., Morais, J., Kolinsky, R., Braga, L. W., Guerreiro-Tauil, A., Dehaene, S., & Cohen, L. (2020). Impact of literacy on the functional connectivity of vision and language related networks. *NeuroImage*, *213*, 116722. https://doi.org/10.1016/j.neuroimage.2020.116722

Ludersdorfer, P., Wimmer, H., Richlan, F., Schurz, M., Hutzler, F., & Kronbichler, M. (2016). Left ventral occipitotemporal activation during orthographic and semantic processing of auditory words. *NeuroImage*, *124*, 834–842.

Murphy, K., & Fox, M. D. (2017). Towards a consensus regarding global signal regression for resting state functional connectivity MRI. *NeuroImage*, *154*, 169–173.

Olulade, O. A., Flowers, D. L., Napoliello, E. M., & Eden, G. F. (2015). Dyslexic children lack word selectivity gradients in occipito-temporal and inferior frontal cortex. *NeuroImage: Clinical*, *7*, 742–754.

Parkes, L., Fulcher, B., Yücel, M., & Fornito, A. (2018). An evaluation of the efficacy, reliability, and sensitivity of motion correction strategies for resting-state functional MRI. *NeuroImage*, *171*, 415–436.

Planton, S., Chanoine, V., Sein, J., Anton, J. L., Nazarian, B., Pallier, C., & Pattamadilok, C. (2019). Top-down activation of the visuo-orthographic system during spoken sentence processing. *NeuroImage*, *202*, 116135. https://doi.org/10.1016/j.neuroimage.2019.116135

Power, J. D., Plitt, M., Laumann, T. O., & Martin, A. (2017). Sources and implications of whole-brain fMRI signals in humans. *NeuroImage*, *146*, 609–625.

Price, C. J., & Devlin, J. T. (2003). The myth of the visual word form area. *NeuroImage*, *19*, 473–481.

Reich, L., Szwed, M., Cohen, L., & Amedi, A. (2011). A ventral visual stream reading center independent of visual experience. *Current Biology*, *21*, 363–368.

Rosenke, M., Van Hoof, R., Van Den Hurk, J., Grill-Spector, K., & Goebel, R. (2021). A probabilistic functional atlas of human occipito-temporal visual cortex. *Cerebral Cortex*, *31*, 603–619.

Saad, Z. S., Gotts, S. J., Murphy, K., Chen, G., Jo, H. J., Martin, A., & Cox, R. W. (2012). Trouble at rest: How correlation patterns and group differences become distorted after global signal regression. *Brain Connectivity*, *2*, 25–32.

Saygin, Z. M., Norton, E. S., Osher, D. E., Beach, S. D., Cyr, A. B., Ozernov-Palchik, O., Yendiki, A., Fischl, B., Gaab, N., & Gabrieli, J. D. E. (2013). Tracking the roots of reading ability: White matter volume and integrity correlate with phonological awareness in prereading and early-reading kindergarten children. *Journal of Neuroscience*, *33*, 13251–13258.

Saygin, Z. M., Osher, D. E., Koldewyn, K., Reynolds, G., Gabrieli, J. D. E., & Saxe, R. R. (2012). Anatomical connectivity patterns predict face selectivity in the fusiform gyrus. *Nature Neuroscience*, *15*, 321–327.

Saygin, Z. M., Osher, D. E., Norton, E. S., Youssoufian, D. A., Beach, S. D., Feather, J., Gaab, N., Gabrieli, J. D. E., & Kanwisher, N. (2016). Connectivity precedes function in the development of the visual word form area. *Nature Neuroscience*, *19*, 1250–1255.

Schurz, M., Wimmer, H., Richlan, F., Ludersdorfer, P., Klackl, J., & Kronbichler, M. (2015). Resting-state and task-based functional brain connectivity in developmental dyslexia. *Cerebral Cortex*, *25*, 3502–3514.

Silver, M. A., & Kastner, S. (2009). Topographic maps in human frontal and parietal cortex. *Trends in Cognitive Sciences*, *13*, 488–495.

Skeide, M. A., Brauer, J., & Friederici, A. D. (2016). Brain functional and structural predictors of language performance. *Cerebral Cortex*, *26*, 2127–2139.

Smith, G. J., Booth, J. R., & McNorgan, C. (2018). Longitudinal task-related functional connectivity changes predict reading development. *Frontiers in Psychology*, *9*, 1754.

Song, Y., Tian, M., & Liu, J. (2012). Top-down processing of symbolic meanings modulates the visual word form area. *The Journal of Neuroscience*, *32*, 12277–12283.

Stevens, W. D., Kravitz, D. J., Peng, C. S., Tessler, M. H., & Martin, A. (2017). Privileged functional connectivity between the visual word form area and the language system. *Journal of Neuroscience*, *37*, 5288–5297.

Stevens, W. D., Tessler, M. H., Peng, C. S., & Martin, A. (2015). Functional connectivity constrains the category-related organization of human ventral occipitotemporal cortex. *Human Brain Mapping*, *36*, 2187–2206.

Stigliani, A., Weiner, K. S., & Grill-Spector, K. (2015). Temporal processing capacity in high-level visual cortex is domain specific. *Journal of Neuroscience*, *35*, 12412–12424.

Taylor, J. S. H., Davis, M. H., & Rastle, K. (2019). Mapping visual symbols onto spoken language along the ventral visual stream. *Proceedings of the National Academy of Sciences of the United States of America*, *116*, 17723–17728.

Tsao, D. Y., Moeller, S., & Freiwald, W. A. (2008). Comparing face patch systems in macaques and humans. *Proceedings of the National Academy of Sciences of the United States of America*, *105*, 19514–19519.

van der Mark, S., Bucher, K., Maurer, U., Schulz, E., Brem, S., Buckelmüller, J., Kronbichler, M., Loenneker, T., Klaver, P., Martin, E., & Brandeis, D. (2009). Children with dyslexia lack multiple specializations along the visual word-form (VWF) system. *NeuroImage*, *47*, 1940–1949.

van der Mark, S., Klaver, P., Bucher, K., Maurer, U., Schulz, E., Brem, S., Martin, E., & Brandeis, D. (2011). The left occipitotemporal system in reading: Disruption of focal fMRI connectivity to left inferior frontal and inferior parietal language areas in children with dyslexia. *NeuroImage*, *54*, 2426–2436.

Vandermosten, M., Boets, B., Poelmans, H., Sunaert, S., Wouters, J., & Ghesquiere, P. (2012). A tractography study in dyslexia: Neuroanatomic correlates of orthographic, phonological and speech processing. *Brain*, *135*, 935–948.

Vinckier, F., Dehaene, S., Jobert, A., Dubus, J. P., Sigman, M., & Cohen, L. (2007). Hierarchical coding of letter strings in the ventral stream: Dissecting the inner organization of the visual word-form system. *Neuron*, *55*, 143–156.

Vogel, A. C., Miezin, F. M., Petersen, S. E., & Schlaggar, B. L. (2012). The putative visual word form area is functionally connected to the dorsal attention network. *Cerebral Cortex*, *22*, 537–549.

Vogel, A. C., Petersen, S. E., & Schlaggar, B. L. (2014). The VWFA: It's not just for words anymore. *Frontiers in Human Neuroscience*, *8*, 1–10.

Wang, L., Mruczek, R. E. B., Arcaro, M. J., & Kastner, S. (2015). Probabilistic maps of visual topography in human cortex. *Cerebral Cortex*, *25*, 3911–3931.

Wang, X., Caramazza, A., Peelen, M. V., Han, Z., & Bi, Y. (2014). Reading without speech sounds: VWFA and its connectivity in the congenitally deaf. *Cerebral Cortex*, *25*(9), 2416–2426.

Weiner, K. S., Barnett, M. A., Lorenz, S., Caspers, J., Stigliani, A., Amunts, K., Zilles, K., Fischl, B., & Grill-Spector, K. (2017). The cytoarchitecture of domain-specific regions in human high-level visual cortex. *Cerebral Cortex*, *27*, 146–161.

Weiner, K. S., & Yeatman, J. D. (2020). The cognitive neuroanatomy of human ventral occipitotemporal cortex. In D. Poeppel, G. R. Mangun, & M. S. Gazzaniga (Eds.), *The cognitive neurosciences* (6th ed., pp. 109–116). MIT Press.

Weiner, K. S., Yeatman, J. D., & Wandell, B. A. (2017). The posterior arcuate fasciculus and the vertical occipital fasciculus. *Cortex*, *97*, 274–276.

White, A. L., Kay, K. N., Tang, K. A., & Yeatman, J. D. (2023). Engaging in word recognition elicits highly specific modulations in visual cortex. *Current Biology*, *33*, 1308–1320.e5.

White, A. L., Palmer, J., Boynton, G. M., & Yeatman, J. D. (2019). Parallel spatial channels converge at a bottleneck in anterior word-selective cortex. *Proceedings of the National Academy of Sciences of the United States of America*, *116*, 10087–10096.

Wise Younger, J., Tucker-Drob, E., & Booth, J. R. (2017). Longitudinal changes in reading network connectivity related to skill improvement. *NeuroImage*, *158*, 90–98.

Yeatman, J. D., Dougherty, R. F., Ben-Shachar, M., & Wandell, B. A. (2012). Development of white matter and reading skills. *Proceedings of the National Academy of Sciences of the United States of America*, *109*, E3045–E3053.

Yeatman, J. D., Dougherty, R. F., Myall, N. J., Wandell, B. A., & Feldman, H. M. (2012). Tract profiles of white matter properties: Automating fiber-tract quantification. *PLoS One*, *7*, e49790.

Yeatman, J. D., Dougherty, R. F., Rykhlevskaia, E., Sherbondy, A. J., Deutsch, G. K., Wandell, B. A., & Ben-Shachar, M. (2011). Anatomical properties of the arcuate fasciculus predict phonological and reading skills in children. *Journal of Cognitive Neuroscience*, *23*, 3304–3317.

Yeatman, J. D., Rauschecker, A. M., & Wandell, B. A. (2013). Anatomy of the visual word form area: Adjacent cortical circuits and long-range white matter connections. *Brain and Language*, *125*, 146–155.

Yeatman, J. D., Weiner, K. S., Pestilli, F., Rokem, A., Mezer, A., & Wandell, B. A. (2014). The vertical occipital fasciculus: A century of controversy resolved by in vivo measurements. *Proceedings of the National Academy of Sciences of the United States of America*, *111*, E5214–E5223.

Yeatman, J. D., & White, A. L. (2021). Reading: The confluence of vision and language. *Annual Review of Vision Science*, *7*, 487–517.

Yeo, B. T., Krienen, F. M., Sepulcre, J., Sabuncu, M. R., Lashkari, D., Hollinshead, M., Roffman, J. L., Smoller, J. W., Zöllei, L., Polimeni, J. R., Fisch, B., Liu, H., & Buckner, R. L. (2011). The organization of the human cerebral cortex estimated by intrinsic functional connectivity. *Journal of Neurophysiology*, *106*, 1125–1165.

Zhan, M., Pallier, C., Agrawal, A., Dehaene, S., & Cohen, L. (2023). Does the visual word form area split in bilingual readers? A millimeter-scale 7-T fMRI study. *Science Advances*, *9*, eadf6140.

Zhou, W., Xia, Z., Bi, Y., & Shu, H. (2015). Altered connectivity of the dorsal and ventral visual regions in dyslexic children: A resting-state fMRI study. *Frontiers in Human Neuroscience*, *9*, 1–10.

SUPPORTING INFORMATION

Additional supporting information can be found online in the Supporting Information section at the end of this article.

How to cite this article: Yablonski, M., Karipidis, I. I., Kubota, E., & Yeatman, J. D. (2024). The transition from vision to language: Distinct patterns of functional connectivity for subregions of the visual word form area. *Human Brain Mapping*, *45*(4), e26655. https://doi.org/10.1002/hbm.26655